LLNL-JRNL-653602

Long-term Sea-Level Change Revisited: The Role of Salinity

P. J. Durack, S. E. Wijffels, P. J. Gleckler

April 23, 2014

Environmental Research Letters

Disclaimer

LONG-TERM SEA-LEVEL CHANGE REVISITED: THE ROLE OF SALINITY

Paul J. Durack[1,2,3], Susan E. Wijffels[2,3] and Peter J. Gleckler[1]

[1]Program for Climate Model Diagnosis and Intercomparison, Lawrence Livermore National Laboratory, Livermore CA, U.S.A.

[2]Centre for Australian Weather and Climate Research, CSIRO Marine and Atmospheric Research, Hobart, Tasmania, Australia

[3]CSIRO Oceans and Atmosphere Flagship, Hobart, Tasmania, Australia

Submitted: Monday, 11 August 14
Abstract: 201 words
Main text: 4061 words (including text, titles and references and excluding figure captions)

Corresponding author address: Paul J. Durack, PCMDI/LLNL, Mail Code L-103, 7000 East Avenue, Livermore, California 94550, U.S.A.
E-mail: pauldurack@llnl.gov

Keywords: oceanography, sea level, salinity, global change, water cycle, climate model, CMIP5

Key points:

- Large-scale salinity-driven halosteric magnitudes can be 25% or more of thermosteric change
- Halosteric changes can counteract or reinforce thermosteric changes
- Climate models reproduce the basin-scale features of observed halosteric changes
- Halosteric patterns provide insights into water cycle and land-ice changes

1. Abstract

Of the many processes contributing to long-term sea-level change, little attention has been paid to the large-scale contributions of salinity-driven halosteric changes. We evaluate observed and simulated estimates of long-term (1950-present) halosteric patterns and compare these to corresponding thermosteric changes. Spatially coherent halosteric patterns are visible in the historical record, and are consistent with estimates of long-term water cycle amplification. Our results suggest that basin-scale halosteric changes in the Pacific and Atlantic are substantially larger than previously assumed, with observed estimates and coupled climate models suggesting magnitudes of ~30% of the corresponding thermosteric changes. In both observations and simulations Pacific basin-scale freshening leads to a density reduction that augments coincident thermosteric expansion, whereas in the Atlantic halosteric changes partially compensate strong thermosteric expansion via a basin-scale enhanced salinity density increase. Although regional differences are apparent, at basin-scales consistency is found between the observed and simulated partitioning of halosteric and thermosteric changes, and suggests that models are simulating the processes driving observed long-term basin-scale steric changes. Further analysis demonstrates that the observed halosteric changes and their basin partitioning are consistent with CMIP5 simulations that include anthropogenic CO_2 forcings (*Historical*), but are found to be inconsistent with simulations that exclude anthropogenic forcings (*HistoricalNat*).

2. Introduction

Changes to global mean sea-level (GMSL) are a well-documented response to a changing climate (Church *et al* 2013a), and many processes associated with sea-level (SL) changes are active areas of research (e.g. Alley *et al* 2005; Velicogna 2009; Stammer 2010; Rignot *et al* 2011; Bouttes *et al* 2012, 2013; Lorbacher *et al* 2012; Brunnabend *et al* 2012; Shepherd *et al* 2012; Wada *et al* 2012; Bouttes and Gregory 2014; Griffies *et al* 2014). However, salinity-driven halosteric patterns of long-term SL change have received relatively little attention. Regional halosteric anomalies have been shown to be important drivers of steric SL variability on short timescales (Pattullo *et al* 1955; Tabata *et al* 1986; Maes 1998; Sato *et al* 2000; Wunsch *et al* 2007; Suzuki and Ishii 2011). However, these changes have been mostly ignored in long-term (>30 year) observed estimates of SL change because halosteric fluctuations (excluding comparatively small mass contributions associated with land-ice changes e.g. Antonov *et al* 2002; Munk 2003; Ishii *et al* 2006) sum to near zero in the global mean (e.g. Gregory and Lowe 2000). Consequently previous GMSL change estimates have primarily considered thermosteric effects along with mass contributions (Church *et al* 2013a).

Estimates of halosteric and thermosteric changes are respectively derived from in-situ observations of salinity and temperature. Previous studies have reported long-term change estimates for ocean salinity (Antonov *et al* 2002; Boyer *et al* 2005; Ishii *et al* 2006; Hosoda *et al* 2009; Durack and Wijffels 2010; Helm *et al* 2010; Durack *et al* 2012, 2013; Skliris *et al* 2014) and temperature (Levitus *et al* 2000, 2005a; Antonov *et al* 2005; Ishii *et al* 2006; Smith and Murphy 2007; Domingues *et al* 2008; Ishii and Kimoto

2009; Gleckler *et al* 2012; Levitus *et al* 2012). There is a general agreement in the broad-scale patterns and magnitudes of salinity and temperature changes among these independent studies. Formal climate change detection and attribution studies (Barnett *et al* 2005; Pierce *et al* 2006, 2012; Pardaens *et al* 2008; Gleckler *et al* 2012) have attributed ocean temperature changes to anthropogenic CO_2 forcing, and the recent studies of Pierce *et al* (2012) and Terray *et al* (2012) have detected an anthropogenic influence which is driving observed ocean salinity changes.

Fewer studies have focused on derived steric changes than on the underlying changes to the salinity and temperature fields. Several observational (e.g. Pattullo *et al* 1955; Tabata *et al* 1986; Maes 1998; Sato *et al* 2000; Antonov *et al* 2002; Levitus *et al* 2005b; Ishii *et al* 2006; Suzuki and Ishii 2011) and ocean reanalysis (e.g. Carton *et al* 2005; Wunsch *et al* 2007; Köhl and Stammer 2008) studies have highlighted the importance of salinity to regionally observed SL. Others have considered the global patterns of projected 21st century SL changes from climate models (Landerer *et al* 2007; Yin *et al* 2010; Pardaens *et al* 2011; Yin 2012; Bouttes and Gregory 2014).

In the present study we extend upon these previous analyses to contrast the relative importance of basin-scale halosteric and thermosteric changes in two independent observational datasets over the period 1950 to 2008, and use these estimates to evaluate the historically forced simulations available from CMIP5 (Taylor *et al* 2012). We show that halosteric patterns can be very important at basin-scales even though they do not contribute to GMSL change.

The paper is organized as follows: in section 2 we describe the observations, model simulations and methods used in this study, in section 3 we compare multi-decadal observed and simulated halosteric and thermosteric trends at basin- to regional-scales. In section 4 we conclude by discussing the implications of this work, touch on the limitations of the present study and outline further work required to better understand large-scale observed and simulated SL changes.

2. Data and methods

To evaluate the long-term halosteric and thermosteric SL changes from CMIP5 Historical simulations (Taylor *et al* 2012), we consider data from two independent observational analyses (Ishii and Kimoto 2009; Durack and Wijffels 2010 - hereafter Ish09 and DW10 respectively).

The Ish09 (Ishii and Kimoto 2009) analysis exploits the full salinity and thermal archive and employs a bias correction scheme in order to utilise problematic eXpendable BathyThermograph (XBT) and Mechanical BathyThermograph (MBT) profiles, that contain well-documented depth and thermister biases (Gouretski and Koltermann 2007*;* Wijffels *et al* 2008*;* Abraham *et al* 2013; Cowley *et al* 2013). This analysis uses an objective mapping technique to generate monthly mean globally gridded salinity and temperature maps for the period 1945-2012. We note that long-term temperature trends (and the corresponding thermosteric patterns) from the Ish09 analysis compare well with other objectively analysed products (e.g. Levitus *et al* 2012; Good *et al* 2014).

The DW10 (Durack and Wijffels 2010) analysis is based on the full salinity archive that is comprised of high-quality Niskin and Nansen (bottle) casts and CTD (conductivity-temperature-depth) profiles of salinity and temperature. As a consequence, while exploiting considerably less data than corresponding temperature-only analyses (CTD/bottle profiles comprise ~30% of the global ocean temperature archive), the results are free from XBT and MBT biases. We note however, that this analysis compares well to other globally integrated estimates of ocean heat content change that use the full temperature archive. The analysis uses a spatial and temporal parametric model, optimized to recover the broad-scale ocean mean structure, the annual and semi-annual cycle (and their spatial gradients) and the multidecadal linear trends from the sparse hydrographic (salinity and temperature) database over 1950-2008. Importantly, this analysis uses the Argo data and exploits the unprecedented spatial and seasonal coverage to best reduce seasonal and spatial sampling bias. In the sparsely observed Southern Hemisphere oceans, the analysis relies on Argo's ability to highly resolve the mean, seasonal and El-Nino Southern Oscillation (ENSO) responses in salinity and temperature, and thus reduces aliasing due to these dominating modes of variability.

The CMIP5 models assessed in this study are a subset of the full suite, as drift correction in the deeper ocean was necessary. Consequently, 27 independent models were assessed and specific details on the model simulations used in this analysis are contained in Table 1.

In order to directly compare the observational trends with those of the CMIP5 models it was necessary to account for model drift (Covey *et al* 2006; Sen Gupta *et al*

2012, 2013). To account for drift, a linear least-squares fit to a contemporaneous 150-year portion of the piControl simulation (1900-2049) was obtained at each grid point in three dimensions, and this drift estimate was then subtracted grid point by grid point from the corresponding forced simulation trend estimate before calculation of steric anomalies was undertaken.

From each observational dataset, 59-year mean climatologies (1950-2008) were constructed along with least-squares linear trends. For models, 55-year mean climatologies (1950-2004) were constructed along with least-squares linear trends. These fields were calculated on the native grid of the available observations or models, from annual means derived from monthly mean data for Ish09 and models that contributed to CMIP5. We note the temporal discrepancy between observed and simulated analyses which is a result of the limitation of CMIP5 Historical simulations which end in 2005 and the DW10 study which is dependent on the modern Argo period (2004-2008) to estimate the mean climatology and seasonal cycle. We investigated this temporal discrepancy using the Ish09 data, and found that the 1950-2008 and 1950-2004 trend maps are very similar. Consequently the observation-model temporal discrepancy does not have much influence on the key conclusions of the study.

Estimates of total steric, thermosteric and halosteric specific volume anomalies (*svan*) were then calculated from all data using the UNESCO equation of state (Millero *et al* 1980; Millero and Poisson 1981):

$$\begin{aligned} svan_{total} &= \rho(S_{\exp}, T_{\exp}, P) - \rho(\overline{S}, \overline{T}, P) \\ svan_{thermosteric} &= \rho(\overline{S}, T_{\exp}, P) - \rho(\overline{S}, \overline{T}, P) \qquad (1) \\ svan_{halosteric} &= svan_{total} - svan_{thermosteric} \end{aligned}$$

where S denotes salinity, T denotes in-situ temperature and P pressure (dbar). In (1) overbars represent the climatological mean and subscript *exp* indicates the climatological values plus trend anomalies obtained from the observations and models. A key advantage of this method is that the nonlinearities in the equation of state are explicitly resolved, rather than calculating halosteric and thermosteric changes independently by using the coincident climatological values and perturbing salinity or temperature individually.

To enable observation and model intercomparison, and the calculation of a multi-model mean (MMM), all fields were regridded to a 2 x 1 (longitude, latitude) degree grid extending from 70°S to 70°N which excludes marginal seas (Mediterranean Sea, Baltic Sea, Red Sea, Persian Gulf, China Seas, Sea of Japan, Java Sea, Banda Sea and Arafura Sea) and vertically interpolated to 18 standard pressure levels (5, 10, 20, 30, 40, 50, 75, 100, 125, 150, 200, 300, 500, 700, 1000, 1500, 1800, 2000 dbar). To fairly compare both observations and models that have differing land/sea masks, after horizontal interpolation an iterative nearest neighbour filling algorithm was employed to infill regions so that the land/sea masks of all analyses were identical.

3. Results

Steric changes: Global perspective

Warming-driven thermosteric expansion (Figure 1 A2 versus B2), like the corresponding changes to ocean heat uptake, is fairly homogenous throughout and between individual basins in the global ocean. There is agreement in the sign of observed estimates nearly everywhere, particularly in the well-sampled Northern Hemisphere, where a relatively larger thermosteric expansion is apparent in the Atlantic and in the western subtropical North Pacific. In the Southern Hemisphere we find agreement along the axis of the Antarctic Circumpolar current. These features are also captured in the CMIP5 MMM (Figure 1 C2), however as expected the MMM result is smoother, with magnitudes smaller than the observations as a result of averaging across simulations with uncorrelated variability. The thermosteric contraction (cooling) in the western subpolar North Pacific and around Australia, though present in the two observational estimates, is largely absent in the MMM. There is less agreement between observations in the Southern Hemisphere with larger magnitude changes apparent in DW10 and the MMM (Figure 1 B2, C2) compared to a muted result in Ish09 (Figure 1 A2). We note that discrepancies between the observations in the Southern Hemisphere are likely due to poor spatio-temporal observational coverage and conservative infilling methods (e.g. Gille 2002, 2008; Gregory *et al* 2004; Gouretski and Koltermann 2007). Discrepancies between the observed and simulated estimates, particularly in the North Pacific, may be in part associated with the unresolved long-term mode of natural variability in observations (e.g. Pacific Decadal Oscillation, PDO;

Mantua *et al* 1997) as agreement exists in the observations however is absent in the MMM.

In both observational estimates large-scale halosteric contraction (increased salinity) is evident across most of the Atlantic and western Indian Oceans, in contrast to expansion (decreased salinity) in the Pacific (Figure 1 A3 versus B3). This basin contrast between halosteric contraction and expansion is also apparent in the MMM (Figure 1 C3), but inter-model agreement greater than 50% is only found in the equatorial and South Pacific regions (no stippling, Figure 1 C3). In the Atlantic, observations express a sign reversal to halosteric expansion for latitudes greater than 50°N. This may be linked to coincident enhancements to precipitation and riverine discharges into the Arctic Ocean, as well as cryospheric contributions (Peterson *et al* 2006; Kwok and Cunningham 2010; Krishfield *et al* 2012; Straneo and Heimbach 2013) or may also be explained by ocean dynamical responses (e.g. Bouttes *et al* 2013), however we do not further investigate potential sources here.

We note that the largest magnitude halosteric and thermosteric changes are often opposite in sign, and therefore lead to a more homogeneous pattern in the resolved total steric changes, a feature particularly prominent in the North Atlantic (Figure 1 A1-C1). This density compensation is not well understood, however mechanisms driving the compensation have been discussed by Mauritzen *et al* (2012) and Bouttes *et al* (2013).

Regional importance of salinity

As noted earlier, GMSL change estimates have mostly neglected halosteric effects, however a number of more recent thermosteric (ocean heat content [OHC]) change estimates have utilised coincident sea surface height (SSH; total steric) in order to better estimate the regional distribution of ocean heat uptake and thermosteric SL changes (Domingues *et al* 2008) or provide OHC change uncertainty estimates (Lyman and Johnson 2008, 2014). However, as shown (Figure 1 A3-C3) we note that halosteric change magnitudes are large enough in many regions that they play an important role in column-integrated total steric volumes and should not be neglected in future SL studies.

To further evaluate the importance of salinity, we present maps that show the contribution of the absolute halosteric change to the sum of absolute thermosteric and halosteric changes. To highlight changes on larger spatial scales and reduce noise associated with the observational estimates, all fields were smoothed before plotting using a 3-point boxcar filter, which is applied to the 1° latitude by 2° longitude grid. These maps show where the halosteric magnitude is less than 30% (orange) or greater than 30% (blue) of the absolute total, with the 30% threshold obtained by comparing basin mean MMM halosteric versus thermosteric values (see observed and simulated basin-scale comparisons in a subsequent section, Figure 4). We note that this is an extremely difficult test, as both change sign and magnitude in three dimensions are combined to provide the grid point value. The spatial disagreement between observations (stippling) due to observational sparsity and differing analysis techniques is apparent, however large-scale similarities exist (Figure 2). Blue regions are shown in the high latitude north Pacific and Atlantic along with the Western equatorial Pacific and southern subtropical Pacific and Indian Ocean, and suggest halosteric changes may in some regions be the leading contributor to total steric change (greater than 50% of the total: dark blue). However, we note that even though correspondence exists between the observed estimates, the differences require further investigation to better understand the influence of data sparsity convolved with unresolved variability.

Regional steric compensation

Previous studies have identified several regional features where counteracting halosteric contraction (increased salinity) and thermosteric expansion (warming) changes occur (e.g. Antonov *et al* 2002; Levitus *et al* 2005b; Ishii *et al* 2006; Lowe and Gregory 2006; Pardaens *et al* 2011; Mauritzen *et al* 2012; Bouttes *et al* 2013; Griffies *et al* 2014). As a result the total steric change is more spatially uniform between and across basins (Figure 1 A1-C1). In observations, examples include the thermosteric expansion (warming) that is partially offset by halosteric contraction (enhanced salinity) in the North Atlantic, and thermosteric contraction (cooling) that is largely offset by halosteric expansion (decreased salinity) in the equatorial and southwestern Pacific. A similar compensation occurs in the eastern Indian Ocean, while in the northwestern Indian Ocean strong halosteric contraction (enhanced salinity) compensates for a strong thermosteric expansion (warming). Another key region where strong compensation occurs is in the subpolar North Atlantic, which shows a halosteric expansion (decreased salinity) and corresponding thermosteric contraction (cooling) in observations (Figure 1). The models exhibit a large spread in the polar and subpolar regions, and the sign of changes in the subpolar North Atlantic is highly variable even between multiple realisations of the same model (not shown). We note that subpolar regions are complicated by the proximity of sea-ice, the influence of which is beyond the scope of this study. Some of the regions where observed halosteric and thermosteric changes compensate are also present in the MMM, but are much weaker than in observations and are likely due to the smoothing that results from averaging across modelled results.

To further investigate the basin-scale consistency in the patterns of thermosteric and halosteric changes, basin zonal means for each observational estimate and the MMM are shown (Figure 3). The sign consistency between the observed and modelled estimates is encouraging, with particularly good broad-scale agreement in the Pacific and Atlantic basins. In the Pacific (Figure 3B), all estimates suggest a freshening-driven halosteric and warming-driven thermosteric expansion is occurring – steric changes that augment. Observations and simulations are also consistent in the Atlantic, however with the opposite signed changes – density compensation through halosteric contraction and thermosteric expansion. For the Southern Hemisphere Pacific and Indian Oceans, both the DW10 and MMM suggest larger halosteric change amplitudes than Ish09, and their corresponding thermosteric changes are approximately equal in both hemispheres. The larger Southern Hemisphere result is not reproduced in Ish09 possibly due to the conservative nature of resolved changes in regions of poor spatial coverage (e.g. Gille 2002, 2008; Gregory *et al* 2004; Gouretski and Koltermann 2007). In the Atlantic (Figure 3C), a strong warming-driven thermosteric expansion and a near basin-wide halosteric contraction approximately half the thermosteric magnitude is present in observations, a feature that is matched by the MMM in the North Atlantic. In the subpolar Atlantic, strong halosteric and thermosteric agreement is present between observations, however the MMM shows an equally large halosteric change of the opposite sign. For the Indian (Figure 3D), the observations and MMM mostly agree in sign of the thermosteric change, with warming across the entire basin. However, due to the presence of marginal seas with strong regional trends (Arabian Sea and Bay of Bengal), there is no agreement in halosteric sign between the observations and MMM north of the equator. In the globally integrated result, reasonably good agreement exists between the observations and MMM (Figure 3A), with the exception of the northern high latitudes. However, these global zonal mean results mask the strong zonal salinity structure within basins as well as the compensation in the halosteric responses within and between basins.

Observed and simulated basin-scale comparisons

To further examine the ability of the CMIP5 suite to simulate the observed basins-scale steric responses, we contrast the Atlantic and Pacific long-term basin mean halosteric trends for the observations, CMIP5 MMM and individual model results (Figure 4A). The joint Pacific and Atlantic basin sign consistency of the MMM with observations (Figure 1 A3, B3 versus C3) is captured in 23 of 27 Historical simulations, with halosteric contraction (increased salinity) in the Atlantic and expansion (decreased salinity) in the Pacific (Figure 4A, grey symbols). In Figure 4 we also include CMIP5 HistoricalNat simulations that exclude anthropogenic CO_2 and aerosol forcing (green symbols), and for halosteric changes these results span all four quadrants of the scatterplot. This contrast between the Historical and HistoricalNat results suggests anthropogenic forcing is required to produce the halosteric basin asymmetry in the Historical simulations, consistent with the recent positive detection and attribution analyses of Pierce *et al* (2012) and Terray *et al* (2012).

We also find that there is substantial agreement between observed and simulated basin contrasts in thermosteric changes (Figure 4B), here with a positive SL contribution in both basins. As with halosteric changes, thermosteric changes in the Historical simulations are in much better agreement with observations than the HistoricalNat simulations, and are again consistent with previous detection and attribution studies (Barnett *et al* 2005; Pierce *et al* 2006, 2012; Pardaens *et al* 2008; Gleckler *et al* 2012).

Interestingly, when comparing the magnitude of the halosteric basin-scale changes to their thermosteric counterparts, we find they are not negligible as previously assumed. In the Atlantic the basin mean halosteric compensation of the thermosteric anomaly for CMIP5 Historical simulations is 38% and may hide local steric expansion. In the Pacific, where the sign of halosteric and thermosteric agree, halosteric changes also contribute 38% to the total steric anomaly.

4. Discussion

Our examination of the observed long-term halosteric contributions to SL suggests that coherent changes throughout the observed ocean depth have occurred at basin-scales during 1950-2008. By contrasting halosteric and thermosteric changes, our findings highlight that salinity contributions to SL changes are important even at basin-scales.

Unlike temperature, observed and simulated basin-scale salinity changes exhibit a dipole response – a freshening Pacific and a saltier Atlantic (Boyer *et al* 2005; Hosoda *et al* 2009; Durack and Wijffels 2010; Helm *et al* 2010; Durack *et al* 2012, 2013; Terray *et al* 2012; Skliris *et al* 2014) – providing a more clearly defined basin-scale fingerprint of change when compared to the relatively homogenous observed upper-ocean warming pattern (Levitus *et al* 2012; Rhein *et al* 2013). Consequently, observed halosteric changes show greater spatial heterogeneity than their thermosteric counterparts (Figure 1 A3, B3 versus A2, B2), and there is good agreement between the observed analyses. This basin contrast of depth-integrated salinity changes is consistent with reported surface salinity pattern amplification and corresponding changes to the water cycle (Hosoda *et al* 2009; Durack and Wijffels 2010; Helm *et al* 2010; Durack *et al* 2012, 2013; Pierce *et al* 2012; Terray *et al* 2012; Skliris *et al* 2014). The inhomogeneous nature of basin-scale ocean salinity changes and the observed enhancement of spatial gradients and basin contrasts provides an opportunity to evaluate historically forced climate model simulations with ocean salinity observations which are largely independent of temperature.

Comparison of observations with CMIP5 simulations suggests anthropogenic forced changes are driving a coherent pattern of broad-scale halosteric (salinity-driven) changes in the world ocean in agreement with past studies (Pierce *et al* 2012; Terray *et al* 2012). These patterns of halosteric change are consistent with previous work that reported near-surface (and subsurface) ocean salinity pattern amplification and associated water cycle change (Boyer *et al* 2005; Hosoda *et al* 2009; Durack and Wijffels 2010; Helm *et al* 2010; Durack *et al* 2012, 2013; Skliris *et al* 2014), however we note that attribution of the processes driving such changes is complex (e.g. Lowe and Gregory 2006; Bouttes *et al* 2012, 2013; Bouttes and Gregory 2014) and not yet well understood. Conversely, simulations that exclude anthropogenic forcing (CO_2 and aerosols; HistoricalNat) over the period of analysis cannot reproduce the pattern of halosteric and thermosteric changes that are captured in observed estimates.

We note that natural variability associated with climate modes can drive measurable changes to regional patterns of ocean surface freshwater fluxes that can influence GMSL on short timescales (Pardaens *et al* 2008; Boening *et al* 2012; Fasullo *et al* 2013; Cazenave *et al* 2014). However, the influence of natural variability is likely reduced in long-term (50-year or longer) observed and modelled change estimates such as those presented in this study (Figure 4). In addition to changes in the surface freshwater fluxes (evaporation minus precipitation; E-P), depth-integrated changes are also influenced by ocean circulation changes that can also be responsible for salinity/freshwater redistribution, or water mass changes attributable to the coincident broad-scale warming (Lowe and Gregory 2006; Durack and Wijffels 2010; Bouttes *et al* 2012, 2013; Bouttes and Gregory 2014).

The current generation CMIP5 climate models do not interactively simulate land-ice changes, and glacier and ice-sheet changes are primarily calculated using offline models (Church *et al* 2013b). The inclusion of these processes is an anticipated improvement for future coupled modelling systems that will be contributing to CMIP6 (Meehl *et al* 2014). Consequently, consideration for such differences must be accounted for during observation-model intercomparison studies and particularly when considering future model projections, as land-ice contributions become a more dominant contributor to GMSL.

Further work is necessary to better understand and quantify the processes responsible for the observed and simulated regional SL changes, and for this idealised ocean-only simulations are a well suited compliment to results from fully-coupled models models (Stammer 2010; Bouttes *et al* 2012, 2013; Durack *et al* 2012; Lorbacher *et al* 2012; Bouttes and Gregory 2014; Griffies *et al* 2014). Additional work is also needed to better understand the complex space-time observational coverage and its impact on estimates of spatially complete steric changes (e.g. Gille 2006; Cheng and Zhu 2014). This is particularly relevant as recent works have highlighted that Southern Hemispheric long-term global ocean heat content and thermosteric change estimates are likely biased low due to the poor spatial coverage of historical observations and current analysis techniques (Gille 2002, 2008; Gregory *et al* 2004; Gouretski and Koltermann 2007).

Our study confirms that halosteric contributions to steric SL changes are non-negligible on regional to basin-scales. This result has not been acknowledged in previous works as most long-term SL change assessments have been largely focused on GMSL change, thereby explicitly excluding the consideration of halosteric effects. The magnitude of halosteric changes suggests that some care is required when using SSH altimetry to infer regional thermosteric or heat content change (Domingues *et al* 2008) or their uncertainties (Lyman and Johnson 2008, 2014), because neglecting halosteric effects may mask (or enhance) regional warming signals (Figure 2).

Our new results also demonstrate that contrasting basin-scale halosteric and thermosteric changes reveals robust signatures in observations, and that the current CMIP5 generation of historically forced climate models capture the integrated basin-scale characteristics of the observed halosteric changes, even in the presence of substantial regional discrepancies.

Acknowledgements. The work of P.J.D and P.J.G from Lawrence Livermore National Laboratory is a contribution to the U.S. Department of Energy, Office of Science, Climate and Environmental Sciences Division, Regional and Global Climate Modeling Program under contract DE-AC52-07NA27344. The Australian Government Department of Environment, the Bureau of Meteorology and CSIRO through the Australian Climate Change Science Program supported the work of S.E.W. We thank J. Durack of the University of California, San Francisco for helpful comments with early drafts of this manuscript. We acknowledge the sources of observed data used in this study: M. Ishii and M. Kimoto (Ish09) and the International Argo Program and the national programs that contribute to it. We acknowledge the World Climate Research Programme's Working Group on Coupled Modeling, which is responsible for CMIP, and we thank the climate modeling groups (listed in Table 1) for producing and making available their model output. For CMIP the U.S. Department of Energy's Program for Climate Model Diagnosis and Intercomparison provides coordinating support and led development of software infrastructure in partnership with the Global Organization for Earth System Science Portals. The DW10 data presented in this study can be downloaded from the CSIRO Ocean Change website at www.cmar.csiro.au/oceanchange. LLNL Release #: LLNL-JRNL-653602.

Competing Interests. The authors declare that they have no competing financial interests

Authors' Contributions. P.J.D. completed the steric analysis. All authors assisted with interpretation and shared responsibility for writing the manuscript

Author information. Correspondence and requests for materials should be addressed to P.J.D (pauldurack@llnl.gov)

References

Abraham, J. P., M. Baringer, N. L. Bindoff, T. Boyer, L. J. Cheng, J. A. Church, J. L. Conroy, C. M. Domingues, J. T. Fasullo, J. Gilson, G. Goni, S. A. Good, J. M. Gorman, V. Gouretski, M. Ishii, G. C. Johnson, S. Kizu, J. M. Lyman, A. M. Macdonald, W. J. Minkowycz, S. E. Moffitt, M. D. Palmer, A. R. Piloa, F. Reseghetti, K. Schuckmann, K. E. Trenberth, I. Velicogna and J. K. Willis (2013) A Review of Global Ocean Temperature Observations: Implications for Ocean Heat Content Estimates and Climate Change. *Reviews of Geophysics*, **51** (3), pp 450-483. doi: 10.1002/rog.20022

Alley, R.B., P.U. Clark, P. Huybrechts and I. Joughin (2005) Ice-Sheet and Sea-Level Changes. *Science*, **310** (5747), pp 456-460. doi: 10.1126/science.1114613

Antonov, J. I., S. Levitus and T. P. Boyer (2002) Steric sea level variations during 1957-1994: Importance of salinity. *Journal of Geophysical Research*, **107**, (C12). doi: 10.1029/2001JC000964

Antonov, J. I, S. Levitus and T. P. Boyer (2005) Thermosteric sea level rise, 1955-2003. *Geophysical Research Letters*, **32**, L12602, doi: 10.1029/2005GL023112

Barnett, T. P., D. W. Pierce, K. M. AchutaRao, P. J. Gleckler, B. D. Santer, J. M. Gregory and W. M. Washington (2005) Penetration of Human-Induced Warming into the World's Oceans. *Science*, **309** (5732), pp 284-287. doi: 10.1126/science.1112418

Boening, C., J. K. Willis, F. W. Landerer, R. S. Nerem and J. Fasullo (2012) The 2011 La Nina: So strong, the oceans fell. *Geophysical Research Letters*, **39** (19), L19602. doi: 10.1029/2012GL053055

Bouttes, N., J. M. Gregory, T. Kuhlbrodt and T. Suzuki (2012) The effect of windstress change on future sea level change in the Southern Ocean. *Geophysical Research Letters*, **39** (23), L23602. doi: 10.1029/2012GL054207

Bouttes, N., J. M. Gregory, T. Kuhlbrodht and R. S. Smith (2013) The drivers of projected North Atlantic sea level change. *Climate Dynamics*, **early online publication**. doi: 10.1007/s00382-013-1973-8

Bouttes, N. and J. M. Gregory (2014) Attribution of the spatial pattern of CO_2-forced sea level change to ocean surface flux changes. *Environmental Research Letters*, **9** (3). doi: 10.1088/1748-9326/9/3/034004

Boyer, T. P., S. Levitus, J. I. Antonov, R. A. Locarnini and H. E. Garcia (2005) Linear trends in salinity for the World Ocean, 1955-1998. *Geophysical Research Letters*, **32**, L01604. doi: 10.1029/2004GL021791

Brunnabend, S.-E., J. Shröter, R. Timmermann, R. Rietbroek and J. Kusche (2012) Modeled steric and mass-driven sea level change caused by Greenland Ice Sheet melting. *Journal of Geodynamics*, **59-60**, pp 219-225. doi: 10.1016/j.jog.2011.06.001

Carton, J. A., B. S. Giese and S. A. Grodsky (2005) Sea level rise and the warming of the oceans in the Simple Ocean Data Assimilation (SODA) ocean reanalysis. *Journal of Geophysical Research: Oceans*, **110** (C9) C09006. doi: 10.1029/2004JC002817

Cazenave, A., H. B. Dieng, B. Meyssignac, K. von Schuckmann, B. Decharme and E. Berthier (2014) The rate of sea-level rise. *Nature Climate Change*, **4** (5), pp 358-361. doi: 10.1038/nclimate2159

Cheng, L. and J., Zhu (2014) Uncertainties of the Ocean Heat Content Estimation Induced by Insufficient Vertical Resolution of Historical Ocean Subsurface Observations. *Journal of Atmospheric and Oceanic Technology*, **31** (6), pp 1383-1396. doi: 10.1175/JTECH-D-13-00220.1

Church, J. A., P. U. Clark, A. Cazenave, J. M. Gregory, S. Jevrejeva, A. Levermann, M. A. Merrifield, G. A. Milne, R. S. Nerem, P. D. Nunn, A. J. Payne, W. T. Pfeffer, D. Stammer, A. S. Unnikrishnan and contributing authors (2013a) Sea Level Change (Chapter 13). In: *Climate Change 2013: The Physical Science Basis. Contribution of Working Group I to the Fifth Assessment Report of the Intergovernmental Panel on Climate Change* [Stocker, T. F., D. Qin, G.-K. Plattner, M. Tignor, S. K. Allen, J. Boschung, A. Nauels, Y. Xia, V. Bex and P. M. Midgley (eds.)]. Cambridge University Press, Cambridge, United Kingdom and New York, NY, USA, pp 1137-1216. doi: 10.1017/CBO9781107415324.026. Available online: http://www.climatechange2013.org/report/full-report/

Church, J. A., D. Monselesan, J. M. Gregory and B. Marzeion (2013b) Evaluating the ability of process based models to project sea-level change. *Environmental Research Letters*, **8** (1), 014051. doi: 10.1088/1748-9326/8/1/014051

Covey, C., P. J. Gleckler, T. J. Phillips and D. C. Bader (2006) Secular trends and climate drift in coupled ocean-atmosphere general circulation models. *Journal of Geophysical Research*, **111** (D3). doi: 10.1029/2005JD006009

Cowley, R., S. Wijffels, L. Cheng, T. Boyer and S. Kizu (2013) Biases in Expendable Bathythermograph Data: A New View Based in Historical Side-by-Side Comparisons. *Journal of Atmospheric and Oceanic Technology*, **30** (6), pp 1195-1225. doi: 10.1175/JTECH-D-12-00127.1

Domingues, C. M., J. A. Church, N. J. White, P. J. Gleckler, S. E. Wijffels, P. M. Barker and J. R. Dunn (2008) Improved estimates of upper-ocean warming and multi-decadal sea-level rise. *Nature*, **453** (7198), pp 1090-1093. doi: 10.1038/nature07080

Durack, P. J. and S. E. Wijffels (2010) Fifty-Year Trends in Global Ocean Salinities and Their Relationship to Broadscale Warming. *Journal of Climate*, **23**, pp 4342-4362. doi: 10.1175/2010JCLI3377.1

Durack, P. J., S. E. Wijffels and R. J. Matear (2012) Ocean Salinities Reveal Strong Global Water Cycle Intensification During 1950 to 2000. *Science*, **336**, pp 455-458. doi: 10.1126/science.1212222

Durack, P. J**.**, S. E. Wijffels and T. P. Boyer (2013) Long-term salinity changes and implications for the global water cycle (Chapter 28). In: *Ocean Circulation and Climate (Second Edition), A 21st Century Perspective*. [Siedler, G., S.M. Griffies, J. Gould and J.A. Church (Eds.)]. Volume 103, pp 727-757, International Geophysics, Academic Press, Elsevier, Oxford OX5 1GB, UK. doi: 10.1016/B978-0-12-391851-2.00028-3

Fasullo, J. T., C. Boening, F. W. Landerer and R. S. Nerem (2013) Australia's unique influence on global sea level in 2010-11. *Geophysical Research Letters*, **40** (16), pp 4368-4373. doi: 10.1002/grl.50834

Gille, S. T. (2002) Warming of the Southern Ocean Since the 1950s. *Science*, **295** (5558), pp 1275-1277. doi: 10.1126/science.1065863

Gille, S. T. (2006) How nonlinearities in the equation of state of seawater can confound estimates of steric sea level change. *Journal of Geophysical Research: Oceans*, **109** (C3), C03005. doi: 10.1029/2003JC002012
Gille, S. T. (2008) Decadal-Scale Temperature Trends in the Southern Hemisphere Ocean. *Journal of Climate*, **21** (18), pp 4749-4765. doi: 10.1175/2008JCLI2131.1

Gleckler, P. J., B. D. Santer, C. M. Domingues, D. W. Pierce, T. P. Barnett, J. A. Church, K. E. Taylor, K. M. AchutaRao, T. P. Boyer, M. Ishii and P. M. Caldwell (2012) Human-induced global ocean warming on multidecadal timescales. *Nature Climate Change*, **2**, pp 524-529. doi: 10.1038/NCLIMATE1553

Good, S. A., M. J. Martin and N. A. Rayner (2014) EN4: Quality controlled ocean temperature and salinity profiles and monthly objective analyses with uncertainty estimates. *Journal of Geophysical Research*, **118** (12), pp 6704-6716. doi: 10.1002/2013JC009067

Gouretski, V. and K. P. Koltermann (2007) How much is the ocean really warming? *Geophysical Research Letters*, **34**, L01610. doi: 10.1029/2006GL027834

Gregory, J.M., H.T. Banks, P.A. Stott, J.A. Lowe and M.D. Palmer (2004) Simulated and observed decadal variability in ocean heat content. *Geophysical Research Letters*, **31**, L15312. doi: 10.1029/2004GL020258

Gregory, J. M. and J. A. Lowe (2000) Predictions of global and regional sea-level rise using AOGCMs with and without flux adjustment. *Geophysical Research Letters*, **27** (19), pp 3069-3072. doi: 10.1029/1999GL011228

Griffies, S. M., J. Yin, P. J. Durack, P. Goddard, S. C. Bates, E. Behrens, M. Bentsen, D. Bi, A. Biastoch, C. W. Böning, A. Bozec, E. Chassignet, G. Danabasoglu, S. Danilov, C. Domingues, H. Drange, R. Farneti, E. Fernandez, R. J. Greatbatch, D. M. Holland, M. Ilicak, W. G. Large, K. Lorbacher, J. Lu, S. J. Marsland, A. Mishra, A. J. G. Nurser, D. Salas y Mélia, J. B. Palter, B. L. Samuels, J. Schröter, F. U. Schwarzkopf, D. Sidorenko, A. M. Treguier, Y. Tseng, H. Tsujino, P. Uotila, S. Valcke, A. Voldoire, Q. Wang, M. Winton and X. Zhang (2014) An assessment of global and regional sea level for years 1993-2007 in a suite of interannual CORE-II simulations. *Ocean Modelling*, **78**, pp 35-89. doi: 10.1016/j.ocemod.2014.03.004

Helm, K. P., N. L. Bindoff and J. A. Church (2010) Changes in the global hydrological-cycle inferred from ocean salinity. *Geophysical Research Letters*, **37**, L18701. doi: 10.1029/2010GL044222

Hosoda, S., T. Suga, N. Shikama and K. Mizuno (2009) Global Surface Layer Salinity Change Detected by Argo and Its Implication for Hydrological Cycle Intensification. *Journal of Oceanography*, **65**, pp 579-596. doi: 10.1007/s10872-009-0049-1

Ishii, M., M. Kimoto, K. Sakamoto and S.-I. Iwasaki (2006) Steric Sea Level Changes Estimated from Historical Ocean Subsurface Temperature and Salinity Analyses. *Journal of Oceanography*, **62**, (2), pp 155-170. doi: 10.1007/s10872-006-0041-y

Ishii, M. and M. Kimoto (2009) Reevaluation of Historical Ocean Heat Content Variations with Time-Varying XBT and MBT Depth Bias Corrections. *Journal of Oceanography*, **65** (3), pp 287-299. doi: 10.1007/s10872-009-0027-7

Krishfield, R. A., A. Proshutinsky, K. Tateyama, W. J. Williams, E. C. Carmack, F. A. McLaughlin and M.-L. Timmermanns. (2012) Deterioration of perennial sea ice in the Beaufort Gyre from 2003 to 2012 and its impact on the oceanic freshwater cycle. *Journal of Geophysical Research*, **119** (2), pp 1271-1305. doi: 10.1002/2013JC008999

Köhl, A. and D. Stammer (2008) Decadal Sea Level Changes in the 50-Year GECCO Ocean Synthesis. *Journal of Climate*, **21** (9), pp 1876-1890. doi: 10.1175/2007JCLI2081.1

Kwok, R. and G. F. Cunningham (2010) Contribution of melt in the Beaufort Sea to the decline in Arctic multiyear sea ice coverage: 1993-2009. *Geophysical Research Letters*, **37** (20), L20501. doi: 10.1029/2010GL044678

Landerer, F. W., J. H. Jungclaus and J. Marotzke (2007) Regional Dynamic and Steric Sea Level Change in Response to the IPCC-A1B Scenario. *Journal of Physical Oceanography*, **37** (2), pp 296-312. doi: 10.1175/JPO3013.1

Levitus, S., J. I. Antonov, J. Wang, T. L. Delworth, K. W. Dixon and A. J. Broccoli (2000) Anthropogenic Warming of Earth's Climate System. *Science*, **292** (5515), pp 267-270. doi: 10.1126/science.1058154

Levitus, S., J. Antonov and T. Boyer (2005a) Warming of the world ocean, 1955-2003. *Geophysical Research Letters*, **32** (2), L02604. doi: 10.1029/2004GL021592

Levitus, S., J. I. Antonov, T. P. Boyer, H. E. Garcia and R. A. Locarnini (2005b) Linear trends of zonally averaged thermosteric, halosteric and total steric sea level for individual ocean basins and the world ocean, (1955-1959)-(1994-1998). *Geophysical Research Letters*, **32** (16), L16601. doi: 10.1029/2005GL023761

Levitus, S., J. I. Antonov, T. P. Boyer, O. K Baranova, H. E. Garcia, R. A. Locarnini, A. V. Mishonov, J. R. Reagan, D. Seidov, E. S. Yarosh and M. M. Zweng (2012) World ocean heat content and thermosteric sea level change (0-2000 m), 1955-2010. *Geophysical Research Letters*, **39**, L10603. doi: 10.1029/2012GL051106

Lorbacher, K., S. J. Marsland, J. A. Church, S. M. Griffies and D. Stammer (2012) Rapid barotropic sea level rise from ice sheet melting. *Journal of Geophysical Research*, **117** (C6), C06003. doi: 10.1029/2011JC007733

Lowe, J. A. and J. M. Gregory (2006) Understanding projections of sea level rise in a Hadley Centre coupled climate model. *Journal of Geophysical Research: Oceans*, **111** (C11), C11014. doi: 10.1029/2005JC003421

Lyman, J. M. and G. C. Johnson (2008) Estimating Annual Global Upper-Ocean Heat Content Anomalies despite Irregular In Situ Ocean Sampling. *Journal of Climate*, **21** (21), pp 5629-5641. doi: 10.1175/2008JCLI2259.1

Lyman, J. M. and G. C. Johnson (2014) Estimating Global Ocean Heat Content Changes in the Upper 1800 m since 1950 and the Influence of Climatology Choice. *Journal of Climate*, **27** (5), pp 1945-1957. doi: 10.1175/JCLI-D-12-00752.1

Maes, C. (1998) Estimating the influence of salinity on sea level anomaly in the ocean. *Geophysical Research Letters*, **25** (19), pp 3551-3554. doi: 10.1029/98GL02758

Mantua, N. J., S. R. Hare, Y. Zhang, J. M. Wallace and R. C. Francis (1997) A Pacific Interdecadal Climate Oscillation with Impacts on Salmon Production. *Bulletin of the American Meteorological Society*, **78** (6), pp 1069-1079. doi: 10.1175/1520-0477(1997)078<1069:APICOW>2.0.CO;2

Mauritzen, C., A. Melsom and R. T. Sutton (2012) Importance of density-compensated temperature change for deep North Atlantic Ocean heat uptake. *Nature Geoscience*, **5** (12), pp 905-910. doi: 10.1038/ngeo1639

Meehl, G. A., R. Moss, K. E. Taylor, V. Eyring, R. J. Stouffer, S. Bony and B. Stevens (2014) Climate Model Intercomparisons: Preparing for the Next Phase. *EOS, Transactions American Geophysical Union*, **95** (9), pp 77-78. doi: 10.1002/2014EO090001

Millero, F. J. C.-T. Chen, A. Bradshaw and K. Schleicher (1980) A new high pressure equation of state for seawater. *Deep Sea Research*, **27A** (3-4), pp 255-264. doi: 10.1016/0198-0149(80)90016-3

Millero, F. J. and A. Poisson (1981) International one-atmosphere equation of state of seawater. *Deep Sea Research*, **28A** (6), pp 625-629. doi: 10.1016/0198-0149(81)90122-9

Munk, W. (2003) Ocean Freshening, Sea Level Rising. *Science*, **300** (5628), pp 2041-2043. doi: 10.1126/science.1085534

Pardaens, A. K., M. Vellinga, P. Wu and B. Ingleby (2008) Large-Scale Atlantic Salinity Changes over the Last Half-Century: A Model-Observation Comparison. *Journal of Climate*, **21** (8), pp 1698-1720. doi: 10.1175/2007JCLI1988.1

Pardaens, A. K., J. M. Gregory and J. A. Lowe (2011) A model study of factors influencing projected changes in regional sea level over the twenty-first century. *Climate Dynamics*, **36** (9-10), pp 2015-2033. doi: 10.1007/s00382-009-0738-x

Pattullo, J. W. Munk, R. Revelle and E. Strong (1955) The Seasonal Oscillation in Sea Level. *Journal of Marine Research*, **14**, pp 88-156

Peterson, B. J., J. McClelland, R. Curry, R. M. Holmes, J. E. Walsh and K. Aagaard (2006) Trajectory Shifts in the Arctic and Subarctic Freshwater Cycle. *Science*, **313** (5790), pp 1061-1066. doi: 10.1126/science1122593

Pierce, D. W., T. P. Barnett, K. M. AchutaRao, P. J. Gleckler, J. M. Gregory and W. M. Washington (2006) Anthropogenic Warming of the Ocean: Observations and Model Results. *Journal of Climate*, **19** (10), pp 1873-1900. doi: 10.1175/JCLI3723.1

Pierce, D. W., P. J. Gleckler, T. P. Barnett, B. D. Santer and P. J. Durack (2012) The fingerprint of human-induced changes in the ocean's salinity and temperature fields. *Geophysical Research Letters*, **39** (21). doi: 10.1029/2012GL053389

Rhein, M., S. R. Rintoul, S. Aoki, E. Campos, D. Chambers, R. A. Feely, S. Gulev, G. C. Johnson, S. A. Josey, A. Kostianoy, C. Mauritzen, D. Roemmich, L. D. Talley, F. Wang and contributing authors (2013) Observations: Ocean (Chapter 3). In: *Climate Change 2013: The Physical Science Basis. Contribution of Working Group I to the Fifth Assessment Report of the Intergovernmental Panel on Climate Change* [Stocker, T. F., D. Qin, G.-K. Plattner, M. Tignor, S. K. Allen, J. Boschung, A. Nauels, Y. Xia, V. Bex and P. M. Midgley (eds.)]. Cambridge University Press, Cambridge, United Kingdom and New York, NY, USA, pp 255-315. doi: 10.1017/CBO9781107415324.010. Available online: http://www.climatechange2013.org/report/full-report/

Rignot, E., I. Velicogna, M. R. van den Broeke, A. Monaghan and J. T. M. Lenaerts (2011) Acceleration of the contribution of the Greenland and Antarctic ice sheets to sea level rise. *Geophysical Research Letters*, **38** (5), L05503. doi: 10.1029/2011GL046583

Sato, O. T., P. S. Polito and W. T. Liu (2000) Importance of salinity measurements in the heat storage estimation from TOPEX/POSEIDON. *Geophysical Research Letters*, **27**, 4. doi: 10.1029/1999GL011003

Sen Gupta, A., L. C. Muir, J. N. Brown, S. J. Phipps, P. J. Durack, D. Monselesan and S. E. Wijffels (2012) Climate Drift in the CMIP3 Models. *Journal of Climate*, **25** (13), pp 4621-4640. doi: 10.1175/JCLI-D-11-00312.1

Sen Gupta, A., N. C. Jourdain, J. N. Brown and D. Monselesan (2013) Climate Drift in the CMIP5 Models. *Journal of Climate*, **26** (21), pp 8597-8615. doi: 10.1175/JCLI-D-12-00521.1

Shepherd, A., E. R. Ivins, G. A, V. R. Barletta, M. J. Bentley, S. Bettadpur, K. H. Briggs, D. H. Bromwich, R. Forsberg, N. Galin, M. Horwath, S. Jacobs, I. Joughin, M. A. King, J. T. N Lenaerts, J. Li, S. R. M. Ligtenberg, A. Luckman, S. B. Luthcke, M. McMillan, R. Meister, G. Milne, J. Mouginot, A. Muir, J. P. Nicolas, J. Paden, A. J. Payne, H. Pritchard, E. Rignot, H. Rott, L. S. Sørensen, T. A. Scambos, B. Scheuchl, E. J. O. Schrama, B. Smith, A. V. Sundal, J. H. van Anglen, W. J. van de Berg, M. R. van den Broeke, D. G. Vaughan, I. Velicogna, J. Wahr, P. L. Whitehouse, D. J. Wingham, D. Yi, D. Young and H. J. Zwally (2012) A Reconciled Estimate of Ice-Sheet Mass Balance. *Science*, **338** (6111), pp 1183-1189. doi: 10.1126/science.1228102

Skliris, N., R. Marsh, S. A. Josey, S. A. Good, C. Liu, R. P. Allan (2014) Salinity changes in the World Ocean since 1950 in relation to changing surface freshwater fluxes. *Climate Dynamics*, **early online publication**. doi: 10.1007/s00382-014-2131-7

Smith, D. M. and J. M. Murphy (2007) An objective ocean temperature and salinity analysis using covariances from a global climate model. *Journal of Geophysical Research*, **112** (C02022). doi: 10.1029/2005JC003172

Stammer, D. (2010) Reply to comment by J.F.R. Gower on “Response of the global ocean to Greenland and Antarctic ice melting” *Journal of Geophysical Research*, **115** (C10). doi: 10.1029/2010JC006457

Straneo, F. and P. Heimbach (2013) North Atlantic warming and the retreat of Greenland’s outlet glaciers. *Nature*, **504** (7478), pp 36-43. doi: 10.1038/nature12854

Suzuki, T. and M. Ishii (2011) Long-term regional sea level changes due to variations in water mass density during the period 1981-2007. *Geophysical Research Letters*, **38** (21), L21604. doi: 10.1029/2011GL049326

Tabata, S., B. Thomas and D. Ramsen (1986) Annual and Interannual Variability of Steric Sea Level along Line P in the Northeast Pacific Ocean. *Journal of Physical Oceanography*, **16** (8), pp 1378-1398. doi: 10.1175/1520-0485(1986)016<1378:AAIVOS>2.0.CO;2

Taylor, K. E., R. J. Stouffer and G. A. Meehl (2012) An Overview of CMIP5 and the Experiment Design. *Bulletin of the American Meteorological Society*, **93** (4), pp 485-498. doi: 10.1175/BAMS-D-11-00094.1

Terray, L., L. Corre, S. Cravatte, T. Delcroix, G. Reverdin and A. Ribes (2012) Near-Surface Salinity as Nature’s Rain Gauge to Detect Human Influence on the Tropical Water Cycle. *Journal of Climate*, **25** (3), pp 958-977. doi: 10.1175/JCLI-D-10-05025.1

Velicogna, I. (2009) Increasing rates of ice mass loss from the Greenland and Antarctic ice sheets revealed by GRACE. *Geophysical Research Letters*, **36** (19), L19503. doi: 10.1029/2009GL040222

Wada, Y., L. P. H. van Beek, F. C. Sperna Weiland, B. F. Chao, Y.-H. Wu and M. F. B. Bierkens (2012) Past and future contribution of global groundwater depletion to sea-level rise. *Geophysical Research Letters*, **39** (9), L09402. doi: 10.1029/2012GL051230

Wijffels, S. E., J. Willis, C. M. Domingues, P. Barker, N. J. White, A. Gronell, K. Ridgway and J. A. Church (2008) Changing Expendable Bathythermograph Fall Rates and Their Impact on Estimates of Thermosteric Sea Level Rise. *Journal of Climate*, **21** (21), pp5657-5672. doi: 10.1175/2008JCLI2290.1

Wunsch, C., R. M. Ponte and P. Heimbach (2007) Decadal Trends in Sea Level Patterns: 1993-2004. *Journal of Climate*, **20** (24), pp 5889-5911. doi: 10.1175/2007JCLI1840.1

Yin, J., S. M. Griffies and R. J. Stouffer (2010) Spatial Variability of Sea Level Rise in Twenty-First Century Projections. *Journal of Climate*, **23** (17), pp 4585-4607. doi: 10.1175/2010JCLI3533.1

Yin, J. (2012) Century to multi-century sea level rise projections from CMIP5 models. *Geophysical Research Letters*, **39** (17). doi: 10.1029/2012GL052947

Tables

TABLE 1. Observational and CMIP5 model datasets (model numbers denote realisation *X* and model physics version *Y*: r*X*i1p*Y*)

		1950-2004	1950-2004	Hist. drift correction
#	Model/Observation	Historical (Obs. version)	HistoricalNat	piControl
	Ishii & Kimoto (2009) – 1950-2008	6.13		
	Durack & Wijffels (2010) – 1950-2008	1.0		
1	ACCESS1-0	1	-	1
2	ACCESS1-3	1-2	-	1
3	CanESM2	1-5	1-5	1
4	CCSM4	1-6	1-2,4,6	1
5	CESM1-BGC	1	-	1
6	CMCC-CESM	1	-	1
7	CMCC-CMS	1	-	1
8	CNRM-CM5	1-10	1-5,8	1
9	CSIRO-Mk3.6.0	1-10	1-5	1
10	EC-EARTH	2-3,5-7,9-10,12,14	-	1
11	FGOALS-s2	1-3	-	1
12	FIO-ESM	1-3		
13	GFDL-CM3	1-5	-	1
14	GISS-E2-H	1-5 (p=1-3)	1-5 (p=1,3)	1 (p=1-3)
15	GISS-E2-H-CC	1	-	1
16	GISS-E2-R	1-6 (p=1,3)	1-5 (p=1,3)	1
17	GISS-E2-R-CC	1	-	1
18	HadGEM2-CC	1-3	-	1
19	HadGEM2-ES	1-4	1-4	1
20	IPSL-CM5A-LR	1-6	1-3	1
21	IPSL-CM5A-MR	1-3	1-3	1
22	IPSL-CM5B-LR	1	-	1
23	MPI-ESM-LR	1-3	-	1
24	MPI-ESM-P	1	-	1
25	NorESM1-M	1-3	1	1
26	NorESM1-ME	1	-	1
27	bcc-csm1-1	2	-	1

Figures

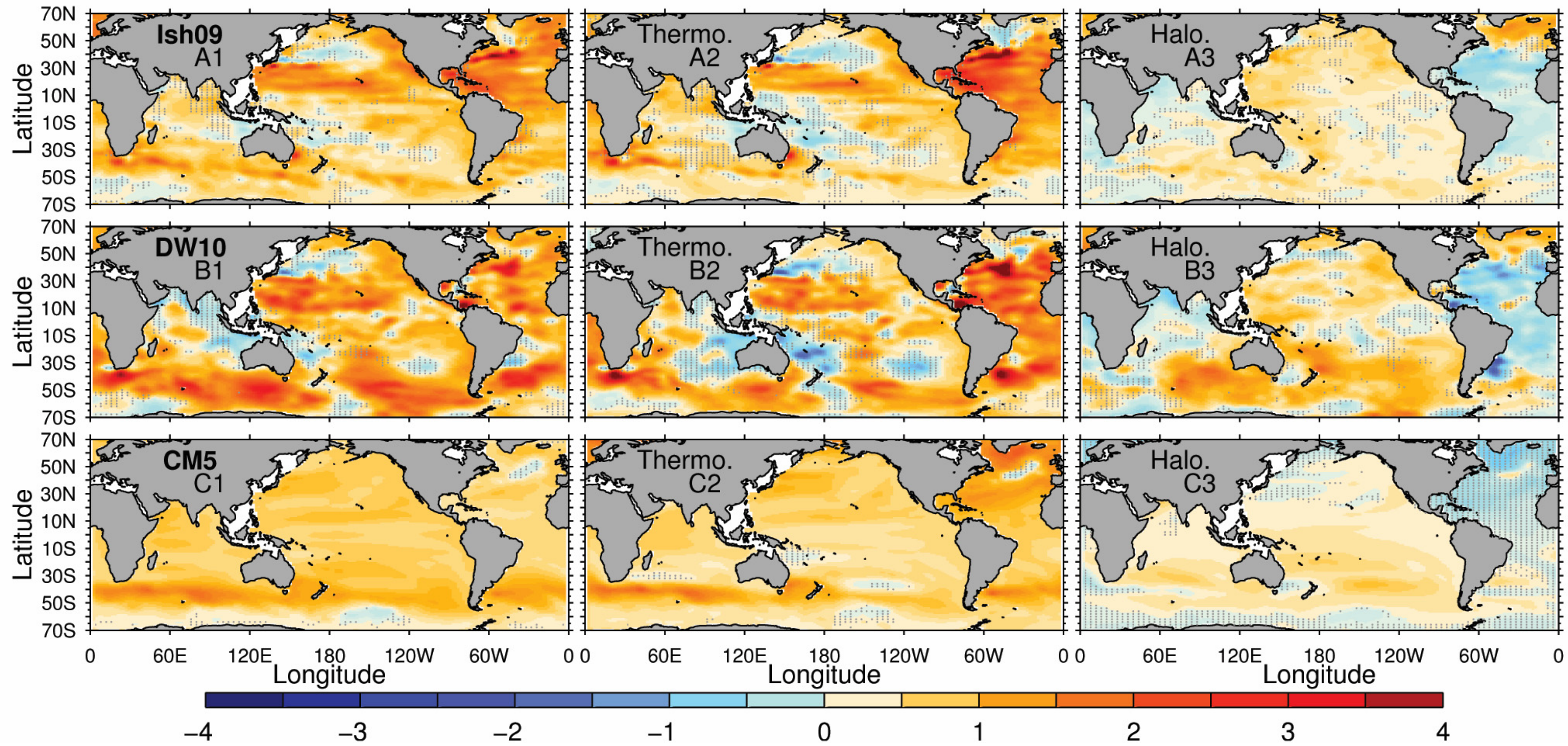

FIG. 1. Long-term trends in 0-2000 dbar total steric anomaly (left column; A1-C1), thermosteric anomaly (middle column; A2-C2) and halosteric anomaly (right column; A3-C3). Units are mm yr^{-1}. Observational maps show results from A) Ishii & Kimoto (2009; 1950-2008), B) Durack & Wijffels (2010; 1950-2008) and C) the CMIP5 Historical multi-model mean (MMM; 1950-2004). Stippling is used to mark regions where the 2 observational estimates do not agree in their sign (A1-A3, B1-B3) and where less than 50% of the contributing models do not agree in sign with the averaged (MMM) map obtained from the ensemble (C1-C3).

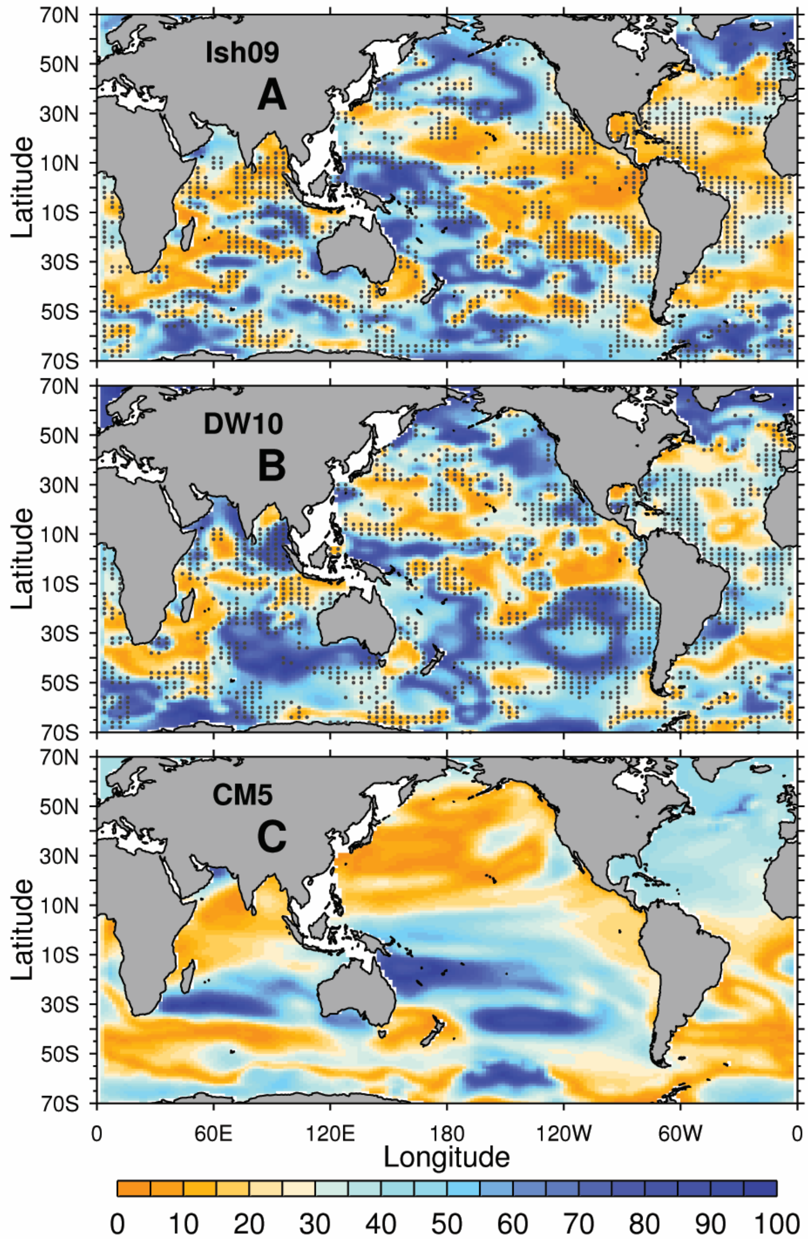

FIG. 2. The magnitude of the 0-2000 dbar column-integrated halosteric changes compared to the integrated absolute steric change (the sum of absolute halosteric and thermosteric changes). Orange colours indicate where the halosteric anomaly comprises 0-30% of the total steric magnitude, whereas blues indicate where halosteric comprises >30%. Stippling is used to mark regions where the 2 observational estimates (A, B) do not agree in their magnitude (either greater than [blue] or less than 30% [orange] which is a threshold obtained from the analysis of basin average halosteric and thermosteric changes [Figure 4]). Observational maps show results from A) Ishii & Kimoto (2009; 1950-2008), B) Durack & Wijffels (2010; 1950-2008) and C) the CMIP5 Historical multi-model mean (MMM; 1950-2004).

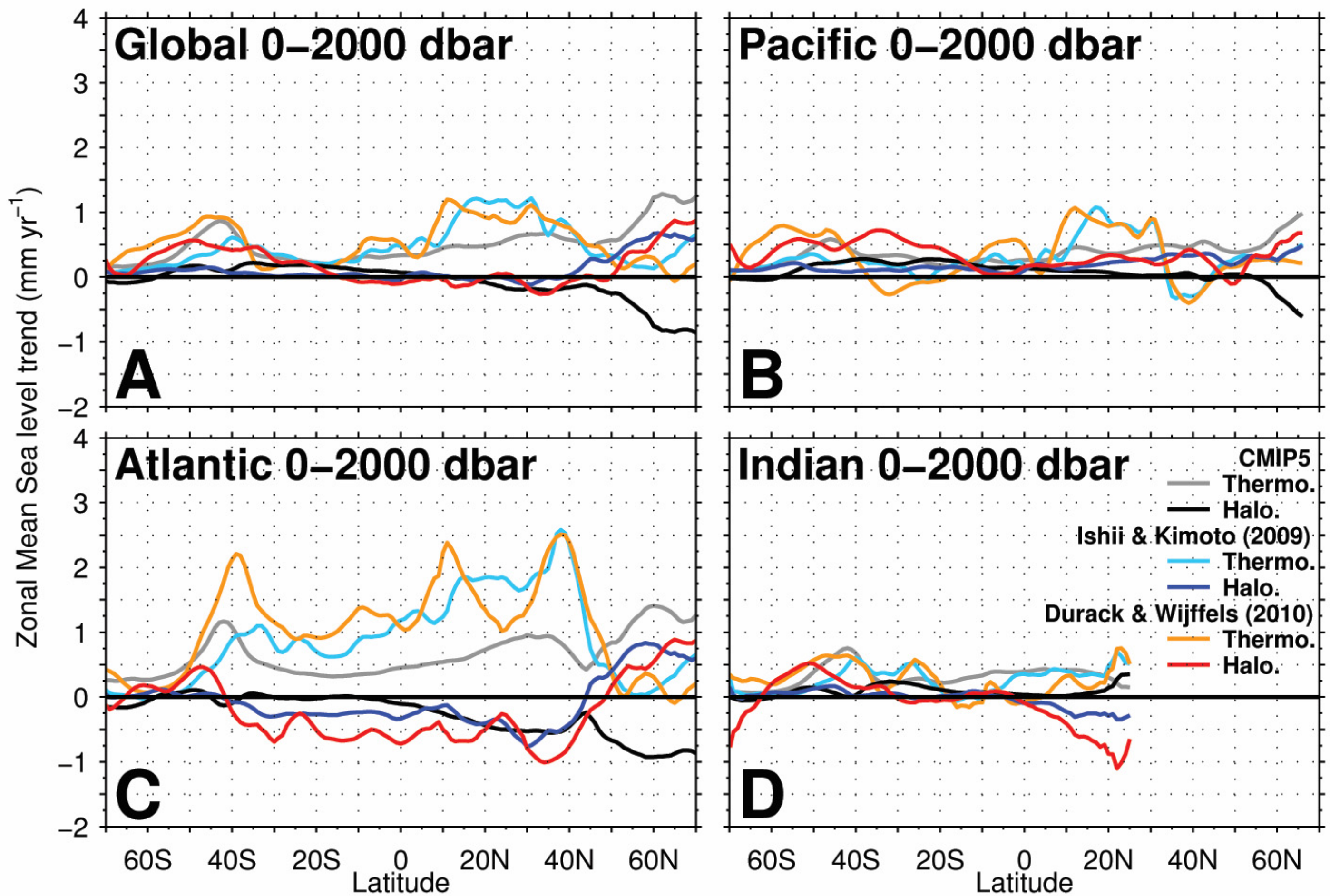

FIG. 3. Zonal mean 0-2000 dbar thermosteric anomaly (light colours) and halosteric anomaly (dark colours) for A) Global, B) Pacific, C) Atlantic and D) Indian Ocean basins. Observational results from Ishii & Kimoto (2009; Light and dark blue, 1950-2008), Durack & Wijffels (2010; Orange and red, 1950-2008) and the CMIP5 Historical multi-model mean (MMM; Grey and black, 1950-2004).

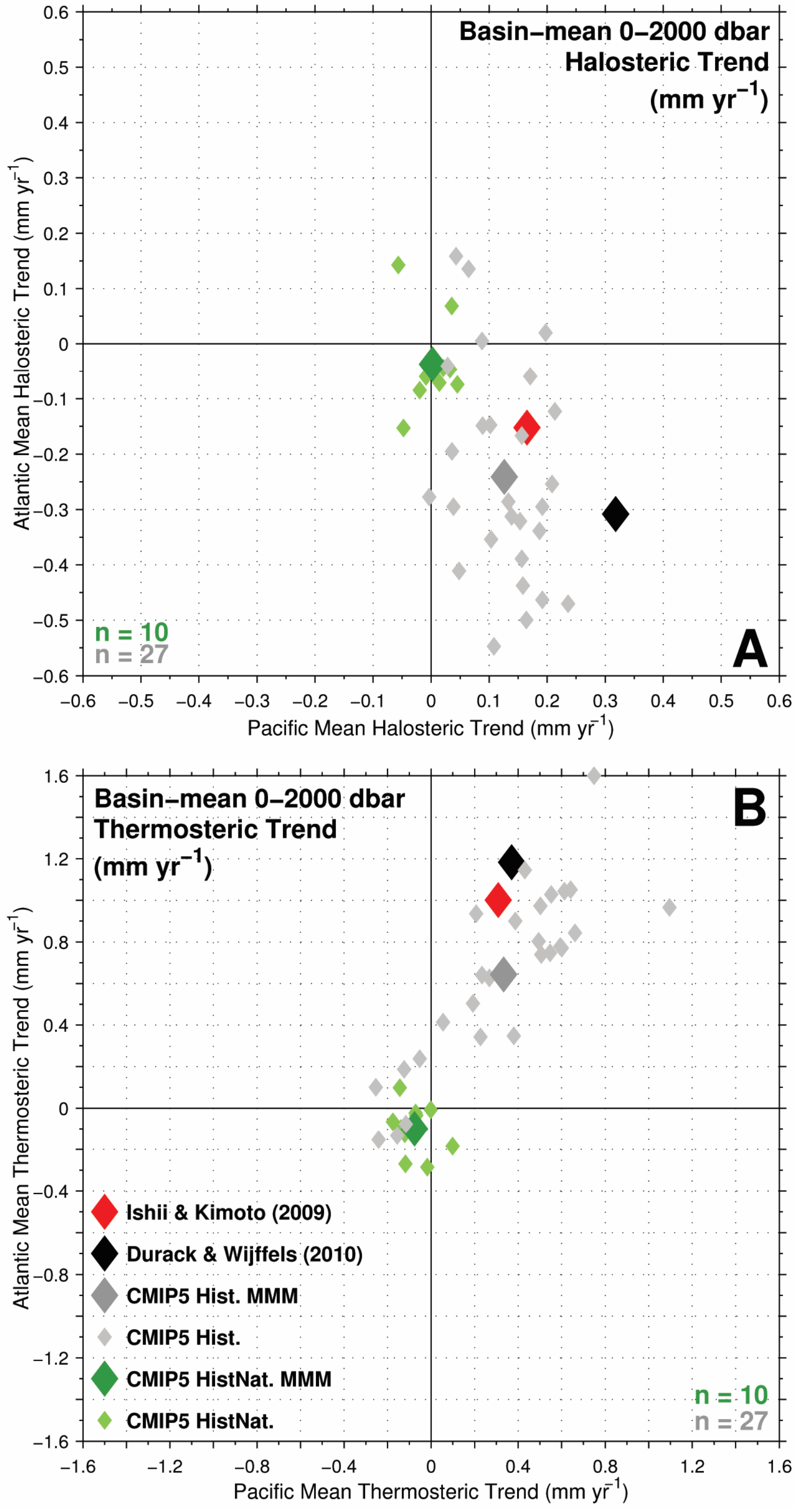

FIG. 4. Area-weighted basin mean 0-2000 dbar A) halosteric and B) thermosteric trends for the Pacific and Atlantic Oceans. Observational results from Ishii & Kimoto (2009; red, 1950-2008), Durack & Wijffels (2010; black, 1950-2008), CMIP5 Historical simulations (grey; 1950-2004) and CMIP5 HistoricalNat simulations (green; 1950-2004).